

Si quantum dots for solar cell fabrication

M. Ficcadenti^{a,*}, N. Pinto^a, L. Morresi^a, R. Murri^a, L. Serenelli^b, M. Tucci^b, M. Falconieri^b, A. Krasilnikova Sytchkova^b, M.L. Grilli^b, A. Mittiga^b, M. Izzi^b, L. Pirozzi^b, S.R. Jadkar^c

^a Department of Physics, University of Camerino, via Madonna delle Carceri, 62032 Camerino, Italy

^b ENEA Research Center Casaccia, via Anguillarese 301, 00123 Rome, Italy

^c Department of Physics, University of Pune, Pune 411007, India

ARTICLE INFO

Article history:

Received 2 May 2008

Received in revised form 21 October 2008

Accepted 24 October 2008

Keywords:

Silicon

Quantum structures

Electrical measurements

Photoconduction

ABSTRACT

Thin film stacks, made of Si-rich SiO alternated with SiO₂ layers, have been deposited by reactive RF sputtering starting from Si and SiO₂ targets, respectively. Crystalline quantum dots (QDs) have been nucleated by Si precipitation from the Si-rich SiO phase using high temperature annealing. PL measurements evidenced a blueshift of the emission peak which has been attributed to a reduction of the Si QD size. Electrical resistivity measurements showed a semiconducting-like behaviour. QD size affect the resistivity values and the activation energies. We have tentatively interpreted the electrical behaviour of this quantum structure by using a Meyer-Neldel Rule conventionally used to explain the electrical properties of nanoporous silicon.

© 2008 Elsevier B.V. All rights reserved.

1. Introduction

In recent years the study of semiconductor quantum structures, such as quantum dots (QDs), has attracted much attention for both fundamental research and device applications. Third generation photovoltaic can take advantage of quantum confinement in silicon.

In particular, when silicon is made very thin in one or more dimensions (less than 20 atomic layers) quantum confinement causes its band gap increase. The strongest effect is obtained in QDs where all three silicon dimensions are reduced. If these QDs are closely spaced together tunnelling of carriers between them can produce QDs superlattices. These last can be used as the top most cell with the highest band gap in the so-called tandem cells.

Several different methods and techniques have been proposed in literature to produce QDs in a dielectric matrix [1,2]. However, a simple approach to prepare multilayers containing silicon QDs has been suggested by Zacharias et al. [1], consisting in the alternating deposition of a silicon rich layer of silicon oxide (SiO_x) followed by a silicon dioxide (SiO₂) layer. High temperature annealing (above 1300 K) of a deposited multilayer, favours the precipitation of silicon and the nucleation of spherical shaped Si nanocrystals, embedded within the SiO₂ matrix. The mean size of the QDs and their distribution in the dielectric matrix host, will depend on the thickness of the SiO_x layer and on the thermal annealing process. Despite the simple deposition approach the physical properties of

the resulting silicon QDs have not been completely explored and understood.

The development of advanced devices based on silicon QD structures requires the investigation and the understanding of the electronic transport, optical and structural properties of these nanostructured material. In particular, the transport properties are also expected to depend on the matrix in which the silicon quantum dots are embedded. In dielectric matrices, the tunnelling between QDs depends on their spacing.

In this paper, we report results of a photoluminescence (PL) and an electrical resistivity investigation of Si QDs embedded in a SiO₂ dielectric matrix. This study can be helpful to design and fabricate an advanced structure of an all Si solar tandem cell.

2. Experimental

Thin film stacks, made of Si-rich SiO alternated with SiO₂ layers, have been deposited by reactive RF sputtering starting from Si and SiO₂ targets, respectively. Films have been deposited both on silicon and quartz in the same deposition run. The choice of the deposition parameters was determined by necessity to guarantee both the desired material stoichiometry and the deposition rate low enough in order to control well the thickness of the growing Si-rich SiO layer. Thus the RF power was 0.55 W/cm² in the case of the Si target and 1.1 W/cm² for the SiO₂ target; the total working pressure was 0.32 Pa and 0.13 Pa, respectively, while the oxygen pressure absolute value of 1×10^{-2} Pa was kept unvaried in both cases, at a fixed position of a leaking valve. Film stoichiometry was checked by X-ray photoelectron spectroscopy (XPS) on a series of calibration

* Corresponding author. Tel.: +39 0737 402528; fax: +39 0737 402853.

E-mail address: marco.ficcadenti@unicam.it (M. Ficcadenti).

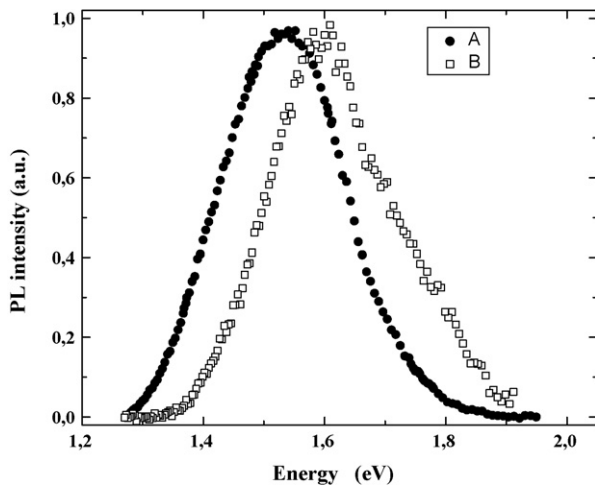


Fig. 1. Normalized photoluminescence of samples A and B, deposited on a silicon and a quartz substrate, respectively. The shoulder above 1.67 eV for sample B is due to a contribution from the quartz substrate.

samples allowing the choice of an adequate oxygen partial pressure for the deposition of the SiO_x layers: $P_{\text{O}_2} = 3\%$ has yielded $x=0.88$.

Crystalline QDs have been nucleated by Si precipitation from the Si-rich SiO phase using high temperature annealing at 1373 K for 60 min in N_2 atmosphere, by using an open tube quartz furnace by Tempress.

Photoluminescence emission spectra were collected by a cooled CCD coupled to a 500 cm focal length monochromator. Samples were excited by a 532 nm frequency-doubled Nd:YAG laser which was fiber-launched into a 32 \times objective also used to collect the signal emitted from the sample in a backscattering geometry. Photoluminescence measurements have been carried out at room temperature, in the wavelength range from about 550 nm to 1000 nm, for samples deposited either on silicon or quartz substrates. PL spectra were not corrected for the system response.

For the electrical characterization, two 0.5 mm apart aluminium contacts, have been evaporated on film surface and then annealed under vacuum ($<10^{-3}$ Pa) conditions at 773 K for 15 h. This procedure ensure an aluminium diffusion through the film down to the quartz substrate [3]. These contacts allows the resistivity measurements of the superlattice in the whole film thickness, parallel to the film surface, i.e. along the multilayers.

In particular, electrical resistivity has been investigated in vacuum condition ($<10^{-3}$ Pa) as a function of the temperature by using an electrometer (Keithley mod. 617) in the V/I mode, by applying a constant dc voltage, in the range of 1–50 V. The temperature has been changed in the range of 300–570 K and the values have been acquired every 5 K, having the sample temperature stabilized within ± 0.1 K with respect to the setting point.

3. Results and discussion

The investigated samples present a PL response in the spectral range from 1.2 eV to about 1.8 eV. Fig. 1 shows the PL for two thermally annealed multilayers, made of 20 periods of $\text{SiO}_x/\text{SiO}_2$, with a nominal thickness of each layer of about 2.4 nm. On the contrary, as-grown multilayers, deposited on a silicon substrate and not thermally annealed, did not evidence any PL emission in the same spectral region.

The broad PL peak, centred at about 1.53 eV, in Fig. 1, is the so-called S-band characterized by a slow decay time and observed in similar systems [4]. The origin of this S-band is still under debate even if several authors believe in a pure quantum confinement

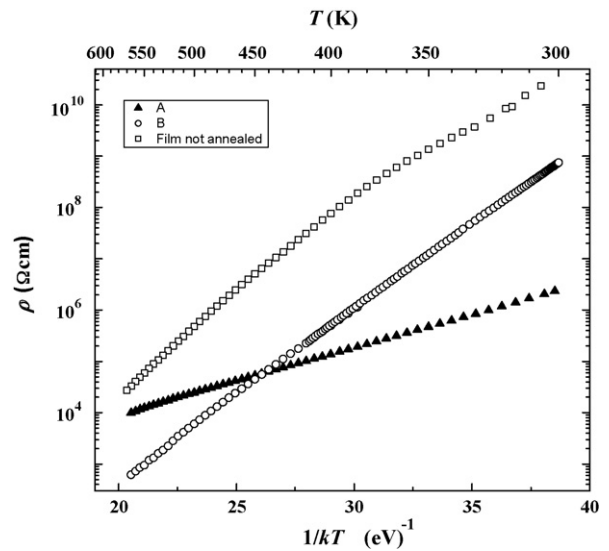


Fig. 2. Resistivity as a function of the energy for multilayer films deposited on quartz. Samples A and B contain QD. For comparison, the figure reproduces the electrical behaviour of a not annealed multilayer, deposited during the same run of sample B.

model in which the emission is due to electron–hole pair recombination [5,6].

For our samples, assuming the quantum confinement model, and comparing the PL peak position with data reported in the literature for similar systems, we estimated for our samples an average Si QD size in the range of 2–3 nm [1,7].

Moreover, the PL peak exhibited by the film A, deposited on a silicon substrate, shows a symmetric shape with a FWHM of about 0.2 eV, lower than that reported by Zacharias et al. of about 0.3 eV and by Green et al. (>0.3 –0.4 eV, depending on the QD size) [1,7]. This suggests a lower QD size dispersion in our samples with respect to data reported in literature, for similar systems.

The PL spectra for the second sample (B), deposited on a quartz substrate, is blueshifted. The PL peak is centred around 1.6 eV and shows a shoulder in the high energy side due to a contribution to the PL signal from the quartz substrate, absent in the spectra collected from the samples deposited on silicon substrates. This contribution has been observed in other films, not reported in the present work. Moreover, the use of a quartz substrate, necessary to investigate the electrical behaviour of films, causes also a decrease of the whole PL intensity, whose origin has not been completely understood. Anyway, the FWHM of sample B is similar to that of the other investigated sample. We have estimated a mean QD size of about 1.5–2.5 nm. The differences in the PL spectra of these two nominally identical samples could be due to a little change in the parameters of the annealing procedure.

The electrical characterization evidenced different behaviour for the annealed and the not annealed multilayer belonging to the same deposition run. Fig. 2 reports the resistivity of the samples A and B, as a function of the temperature, in the range of 300–570 K, and that of the not annealed sample. This last exhibits a very high value at RT, near the sensitivity limit of the electrometer, which exponentially decreases with increasing temperature. Around 400 K, the resistivity (ρ) curve changes its slope. In particular we have found out two activation energies: 0.60 eV, in the range from RT to 390 K, and 0.92 eV in the range from 400 K to 570 K. The electrical behaviour of the not annealed sample is the typical one of an amorphous semiconducting material, similar to those observed in a-Si:H [14]. The measured energies, in the not annealed sample, could correspond to two different transport mechanisms involving transitions among states in the mobility gap of the semiconductor [8].

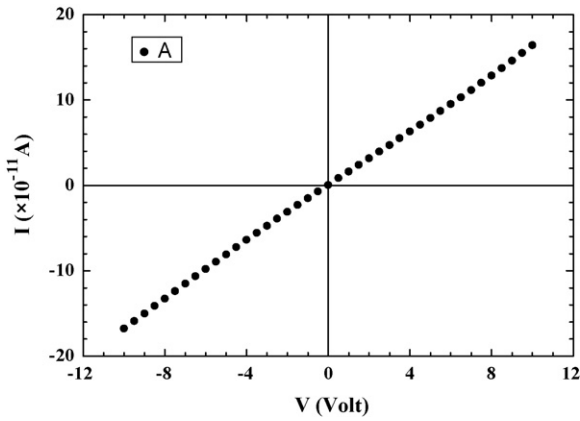


Fig. 3. Current–voltage characteristics at room temperature of sample A.

The resistivity exhibited by the two samples A and B, containing silicon QDs, shows some features related to the presence of silicon QDs in the SiO₂ matrix. The general behaviour is that of a thermally activated process as observed in the not annealed sample. However, resistivity values decrease between two and six orders of magnitude, with the raise of the temperature and the curves change their slope. In detail, sample B shows a RT ρ value of $7 \times 10^8 \Omega \text{ cm}$ which decreases to $6 \times 10^2 \Omega \text{ cm}$ at 570 K, leading to an activation energy of 0.765 eV. In the sample A, the resistivity decreases from $2 \times 10^6 \Omega \text{ cm}$ to about $10^4 \Omega \text{ cm}$, at RT and 570 K, respectively, with an activation energy of about 0.30 eV. In both samples, the activation energy tends to slightly increase above 500 K.

Effects related to tunnelling processes have not been evidenced in our electrical characterization. In fact, considering the contact geometry and the values of the voltages applied to the film, the maximum intensity of the applied electric field was about 10^3 V/m , for $V=50 \text{ V}$. This field intensity is much lower than that needed to the direct tunnelling of electrons through the SiO₂ dielectric barrier, occurring at field intensities much higher than 10^6 V/m [9]. This conclusion agrees with the result of a current–voltage (I – V) characteristics, carried out on our samples and reported in Fig. 3 for the sample A. The I – V characteristics is linear and there are no peaks due to negative resistance effects which can be commonly ascribed to tunnelling processes of electrons in the QDs [10].

To our best knowledge, a model to explain the electronic transport properties in film containing QD is still lacking. However, experimental data interpretation can be tentatively done considering the analogies of our system with the nanoporous silicon one. This last has a coral-like structure the members of which include single nano-crystallites, in the nanometer range. The nano-crystallites form a network of disconnected quantum dots [11]. With the QD size reduction, the PL curves blueshift. The nano-crystallites are considered wrapped by a continuous shell which consists of disordered silicon and silicon oxide [12,13]. In particular, for this last system, Lubianiker and Balberg [14] have suggested two Meyer-Neldel Rules (MNR) to explain all the published data about the electrical conductivity of the porous silicon (PS). The MNR takes into account the relation between the pre-exponential factor of the conductivity (σ) equation, valid for an amorphous semiconductor such as a-Si:H, and the activation energy, E_a :

$$\sigma = \sigma_0 \exp \left[-\frac{E_a}{kT} \right] \quad (1)$$

For the PS, Lubianiker and Balberg [14] demonstrated the existence of only two different conduction mechanisms. One is associated with extended states transport, similar to that one found in a-Si:H,

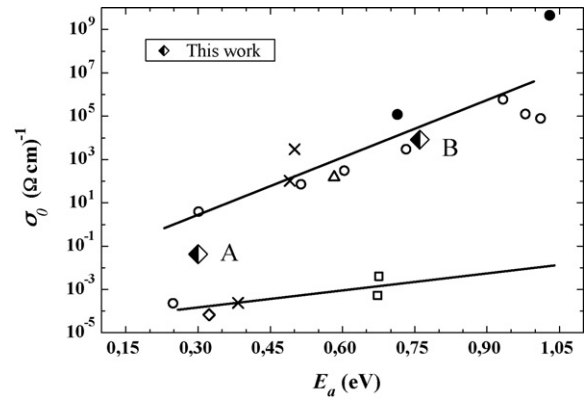


Fig. 4. DC conductivity pre-exponential factor as a function of the corresponding activation energy in a variety of porous silicon samples. Data quoted in the figure have been determined experimentally and they have been taken from Fig. 2 of Ref. [13]. The solid lines represent the best fit to a MNR (see text), for transport in extended states (upper line), and for transport by activated hopping (lower line). The figure also reproduces the results of the present work for the samples A and B.

and the other is associated with activated intra-crystallite hopping. These two different mechanisms are characterized by two well-separated groups of values for σ_0 and E_a . These two groups have been reported in Fig. 4. Assuming the validity of similar arguments for our samples, made of QDs embedded in a dielectric matrix, we have computed the prefactor value, σ_0 , and plotted in the same Fig. 4.

As evident from Fig. 4, sample B presents a σ_0 value which falls in the first group whose conduction mechanism has been suggested to be due to extended states transport [14]. However, the activation energy and the corresponding σ_0 value for the sample B ($E_a = 0.765 \text{ eV}$, $\sigma_0 = 8.3 \times 10^3 \Omega \text{ cm}^{-1}$), is lower than that observed in nanoporous silicon ($E_a = 1.03 \text{ eV}$, $\sigma_0 = 1.4 \times 10^9 \Omega \text{ cm}^{-1}$, see the full circle in Fig. 4) with an average diameter of crystallites about 4 nm.

For sample A, the position of the σ_0 value in Fig. 4 does not allow to make a clear conclusion about the conduction mechanism involved. This sample does not belong to any of the two mentioned groups. This suggests the possible existence of an additional conduction process in between the two mentioned above. Actually this mechanism has not been clearly identified and it will require further investigation.

The above-mentioned differences in the two samples with respect to the results of Lubianiker et al. for PS, could be due to a over simplification of the conduction model invoked to explain the electrical properties. Anyway, we observed a tendency to a little increase of the activation energy with the raise of the temperature as reported by Lee and Lee [15].

Results about the electrical transport properties of our films, are in qualitative agreement with those of Green et al., for multilayer films with a similar structure [7]. In particular, Green et al. reported a lowering of the activation energy of the ρ curve with the increase of the mean QD size. Anyway a more direct comparison cannot be done due to the lack of structural information on our films.

It is important to evaluate the performances of such a multilayer, once it is inserted in a working solar cells. We have therefore tried to estimate the mobility-lifetime product of the photogenerated carriers measuring both the multilayer absorbance $A(\lambda)$ by using a spectrophotometer and the spectral photocurrent $I_{ph}(\lambda)$. An equation for the mobility-lifetime product can be easily obtained starting from the Ohm's law applied to the sample photoconductivity ($I_{ph} = \Delta\sigma V_{bias} S/L$) and from the generation rate expression $G = \Phi_{ph} A(\lambda)/LS$ where S is the photoconductor section, V_{bias} is the applied voltage (100 V), L is the distance between the two contacts (0.5 mm in our sample) and Φ_{ph} is the photon flux. Since $\Delta\sigma = G\tau q\mu$

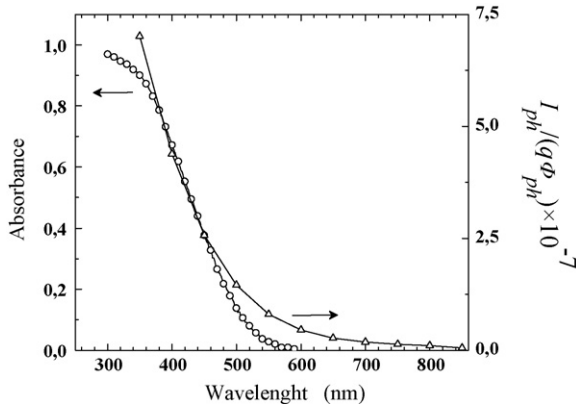


Fig. 5. Spectral photoconductivity normalized to the incident photon flux (triangles and right scale) compared with the multilayer absorbance (circles and left scale). The two curves show a similar behaviour and from their ratio a mobility-lifetime of the photogenerated carriers of the order of $2 \times 10^{-11} \text{ cm}^2/\text{V}$ can be deduced. Continuous lines are only guide to eyes.

we can write:

$$\mu\tau = \frac{I_{ph}}{q\Phi_{ph}A} \frac{L^2}{V_{bias}} \quad (2)$$

In Fig. 5, are reported both $I_{ph}(\lambda)/(q\Phi_{ph})$ and $A(\lambda)$ which show a similar behaviour as expected. From their ratio a mobility-lifetime of the photogenerated carriers of the order of $2 \times 10^{-11} \text{ cm}^2/\text{V}$ is deduced. From this value and using a field of 10^5 V/cm , a drift length of 20 nm results which is still almost an order of magnitude too low for a good collection of photogenerated carriers in a *p-i-n* junction.

4. Conclusions

In this work we have investigated the photoluminescence and the electrical resistivity of two stacked multilayer films containing QDs embedded in a SiO_2 matrix. From PL peak position we extrap-

olated the average size of QDs in our films while the blueshift of the PL curve has been assumed as a reduction of QD mean size. The resistivity evidenced a semiconducting behaviour, with a decrease of the RT value with the raise of the mean QD size. Our investigation evidenced the existence of two possible different conduction mechanisms one of which has been ascribed to a transport in extended states in analogy with a similar mechanism invoked in PS. The second mechanism has not been clearly yet identified and requires further investigations.

References

- [1] M. Zacharias, J. Heitmann, R. Scholz, U. Kahler, M. Schmidt, J. Bläsing, Appl. Phys. Lett. 80 (2002) 661.
- [2] Z.T. Kang, B. Arnold, C.J. Summers, B.K. Wagner, Nanotechnology 17 (2006) 4477–4482.
- [3] M.A. Green, G. Conibeer, Nanostructured silicon-based tandem solar cells, GCEP Technical Report, 2006.
- [4] X. Wen, L. Van Dao, P. Hannaford, J. Phys. D: Appl. Phys. 40 (2007) 3573–3578.
- [5] C. Garcia, B. Garrido, P. Pellegrino, R. Ferre, J.A. Moreno, J.R. Morante, L. Pavesi, M. Cazzanelli, Appl. Phys. Lett. 82 (2003) 1595.
- [6] I. Sychugov, R. Juhasz, J. Valenta, A. Zhang, P. Pirouz, J. Linnros, Appl. Surf. Sci. 252 (2006) 5249.
- [7] M.A. Green, G. Conibeer, E.-C. Cho, D. König, S.J. Huang, D. Song, G. Scardera, Y.-H. Cho, X.J. Hao, T. Fangsuwannarak, S.W. Park, I. Perez Wurfl, Y. Huang, S. Cheng, E. Pink, D. Bellet, E. Bellet-Amalric, T. Puzzer, Proceedings of the 22nd European Photovoltaic Solar Energy Conference, Milan, Italy, 2007, p. 1.
- [8] V. Augelli, R. Murri, JNCS 57 (1983) 223.
- [9] D.J. Di Maria, D.W. Dong, C. Falcony, T.N. Theis, J.R. Kirtley, J.C. Tsang, D.R. Young, F.L. Pesavento, S.D. Brorson, J. Appl. Phys. 54 (1983) 5801.
- [10] G. Coniber, M.A. Green, R. Corkish, Y. Cho, E.C. Cho, C.W. Jiang, T. Fangsuwannarak, E. Pink, Y. Huang, T. Puzzer, T. Trupke, B. Richards, A. Shalav, K. Lin, Thin Solid Films 511–512 (2006) 654–662.
- [11] R. Tsu, D. Bibic, Appl. Phys. Lett. 64 (1994) 1806.
- [12] R. Shinar, D.S. Robinson, J. Partee, P.A. Lane, J. Shinar, J. Appl. Phys. 77 (1995) 3403.
- [13] Y. Lubianiker, I. Balberg, G. Morell, R.S. Katiyar, S.Z. Weisz, Proceedings of the 22nd International Conference on the Physics of Semiconductors, Singapore, 1994, p. 2129.
- [14] Y. Lubianiker, I. Balberg, Phys. Rev. Lett. 78 (1997) 2433.
- [15] W.H. Lee, C. Lee, Proceedings of the 16th International Conference on Amorphous Semiconductors Science and Technology, Kobe, Japan, 1995, p. 374 (Book of Abstracts).